J. Innovative Eng. Nat. Sci., vol. 4, no. 2, pp. 495-513, 2024.
http://doi.org/10.61112/jiens.1445518

JIENS
Journal of Innovative Engineering and Natural Science
(Yenilikçi Mühendislik ve Doğa Bilimleri Dergisi)
https://dergipark.org.tr/en/pub/jiens
Original Paper

A comparative assessment of artificial neural network and regression models to predict mechanical properties of continuously cooled low carbon steels: an external data analysis approach

Emre Alan[a,c]*, İ. İrfan Ayhan[a], Bilgehan Ögel[b] and Deniz Uzunsoy[c]

[a]*ÇEMTAŞ Çelik Mak. San. Tic. A. Ş., R&D Center, Bursa, 16140, Turkey.*
[b]*Middle East Technical University, Dept. of Metallurgical and Materials Eng., Ankara, 06800, Turkey.*
[c]*Bursa Technical University, Dept. of Metallurgical and Materials Eng., Bursa, 16310, Turkey.*

ARTICLE INFO

Article history:
Received 1 March 2024
Received in revised form 14 May 2024
Accepted 23 June 2024

Available online

Keywords:
Artificial neural network
Multiple linear regression
Continuous cooling
Low carbon steel
Mechanical properties

ABSTRACT

In this study, mechanical properties of continuously cooled low carbon steels were predicted via Artificial Neural Network (ANN) and Multiple Linear Regression (MLR) models. Unlike the previous studies, laboratory scaled self-generated data that consists of chemical compositions and cooling rates were used as input while yield strength (YS), ultimate tensile strength (UTS) and total elongation (TE) were served as target data. The prediction performances of the models were compared by applying new data set extracted from external sources like previously studied research papers, thesis or dissertations. A better agreement between predicted and actual data was achieved with ANN model. Additionally, the response of ANN model to new external data resulted in lower prediction errors even the data has one or more input value that is not included in the range of training data set. Unlike ANN model, MLR model shows a significant decrease in prediction accuracy when input data has non-uniform distribution or target data takes place in relatively narrow range. In general, it was shown that ANN model trained with self-generated data can be used as an efficient tool to estimate mechanical properties of continuously cooled low carbon steels that are produced with various conditions, even for the phenomena between input and output is complex and data distribution is non-uniform.

I. INTRODUCTION

Over the last several decades, many attempts have been made in automotive industry to develop new Advanced High Strength Steel (AHSS) grades to meet the rising demands of both increasing passenger safety and decreasing fuel consumption by reducing vehicle's weight. Previous works showed the successful applications of low carbon AHSS grades to satisfy these needs with their combination of high strength and toughness properties [1-3]. Recently, in addition to new material developments studies, steel producers deal with reducing carbon emissions arising from production steps to cope with climate changes. Continuous cooling process is one of the promising candidates to reduce carbon emissions with eliminating the need of additional heat treatments [4-6]. Therefore, research and development studies in steelmaking field focus on developing alternative new continuously cooled low carbon AHSS grades in order to fulfill these tasks in common.

Chemical composition and heat treatment conditions are the main parameters that effect mechanical properties of steel through arranging its microstructure. It is possible to obtain various strength and toughness values for the same steel by applying combinations of different alloy designs and heat treatment routes. Generally, laboratory scaled productions are performed for determining optimum parameters before scaling up to industrial productions. However, a large number of trials usually needs to be done to obtain satisfying results. Even for the laboratory

*Corresponding author. Tel.: +90-555-508-0700; e-mail: ealan@cemtas.com.tr

scaled productions, this requirement brings along time consuming and high cost operations. On the other hand, increasing the number of trials provides the researchers generating a database consists of varying production parameters and test results. In such a case, statistical, mathematical or computational modelling comprise effective solutions on deciding the best option available before physical trials.

Multiple Linear Regression (MLR) is one of the simplest and the most frequently used statistical-based models to predict the changes of a dependent outcome in accordance with at least two independent variables. It is being extensively applied to find the relationships between the properties of steel material and its mechanical performance in service conditions. Estimating the strength or hardness of steel based on its chemical composition is the most studied case on this subject [7-9]. In addition to chemical composition, the process parameters of hot rolling and heat treatment have also been used in some other MLR based studies as predictor variables [10, 11].

In general, traditional statistical regression models have some limitations when calculated phenomena is complex and non-linear [12, 13]. In such cases, Artificial Neural Network (ANN) is a quite useful approach for solving non-linear problems and has a wide usage in steelmaking processes such as estimating the properties of liquid steel and slag [14], optimizing continuous casting [15] and rolling process parameters [16]. ANN is also an effective technique for predicting material properties like critical transformation temperatures [17], continuous cooling transformation (CCT) diagrams [18] and microstructural classifications [19].

The successful applications of ANN for estimating mechanical properties of steel via using various material properties as input data have also been reported in previous studies. Lee et al. [20] designed an ANN model to predict tensile properties of steels based on the fraction of microstructural constituents such as polygonal ferrite, granular bainite, and bainitic ferrite. Yemelyanov et al. [21] developed an ANN model with multi-layered structure to determine mechanical properties of steel. The neurons of input layer were consisted of the amount of different non-metallic inclusions in addition to phase fractions. High performance of model was confirmed with calculated low error values. Saravanakumar et al. [22] proposed an ANN-based model to predict mechanical properties of IS1079 grade low carbon steel by applying hot rolling process parameters and model results were found to be almost same as the measured values. Somkuvar [23] developed an ANN that effectively predicts the hardness of low carbon steel by introducing austenitization temperature and holding time. Fujita et al. [24] used chemical compositions and forging process parameters for training an ANN model in order to estimate hardness distributions and results were compared with finite element method (FEM) calculations. They have reported that ANN approach is more suitable in situations where several phenomena such as metallurgical ones are involved.

In neither of these cases discussed above, the prediction model was developed by using self-generated data nor the performance of models were analyzed by using external data which were extracted from other sources like experimental studies in previous works, data provided from another facilities, etc. Unlike the previous studies related with estimation of mechanical properties of steels, in this study, the self-generated data derived from laboratory scaled productions were used. These data were collected from several R&D projects related with development of continuously cooled low carbon AHSS grades conducted in a steelmaking company. Firstly, MLR model proposed to predict mechanical properties of steels depending on the changes in chemical composition and cooling rates. It is found that MLR method provides faster and accurate solutions when the relationships between predictor and response variables are linear and distribution of data is uniform. However, MLR model falls short of desired performance when the phenomena is complex and needs to be evaluated by taking into consideration of

all dependent parameters. Then, the studies were carried out with ANN based model approach by using the same variables and it is seen that a better correlation can be obtained between predicted and actual values, even the distribution of data is non-uniform and there are non-linear relations between the predictor variables. Moreover, a comparative assessment of MLR and ANN models with external data set has been performed. Performance results showed that the response of ANN model to new external data have a better agreement with actual values compared to MLR model. It is accepted as a common knowledge that a small sized data set in training stage of ANN model results in a poor approximation (14, 25). In this study, it is shown that compared to MLR model, ANN model has not only better performance on predicting mechanical properties of continuously cooled low carbon steels but also its prediction accuracy can be enhanced by increasing the number of data with introducing external data set. It is thought that improved prediction capabilities offers a good opportunity for reducing the production costs and the required time by minimizing the need of plant trials for new material development studies.

II. MATERIALS AND METHODS

2.1 Experimental Alloys

Laboratory scaled vacuum induction melting unit was used for producing experimental heats with various chemical compositions. Industrially produced special steel products were used as raw material for laboratory scaled melting process. Since the raw materials used in this study have already been produced by degassing while their industrial production, the purpose of using vacuum cabinet in laboratory scaled productions was to ensure prevention of re-oxidation during re-melting and casting stages. Therefore, all the melting and casting processes were performed under a vacuum pressure of 20 mbar. Together with the steel raw material, required amount of ferro additions were added to meet the desired chemical compositions. Sectional dimensions of 80x80 mm ingots were cast and homogenization heat treatment was applied at 1200 °C for 2 h. The chemical compositions of steel ingots were analyzed via optical emission spectroscopy (OES) method. The ingots were re-heated at 1150 °C for 45 mins., and then hot deformed into 45x45 mm by using 120-ton capacity hydraulic press. The deformation process consisted of sequenced three steps and 32% of reduction ratio was applied within each step. The final temperature of deformed samples was measured between 914 – 920 °C. After deformation stage, the deformed samples were continuously cooled to room temperature. In order to obtain various cooling rates, fan controlled air cooling unit was used with applying different cooling fan speeds. Cooling regime of each sample was measured and recorded by using a K-type thermocouple with data logger. The production route for this study is shown in Figure 1.

Mechanical properties of continuously cooled productions were obtained via uniaxial tensile test. Yield strength (YS), ultimate tensile strength (UTS) and total elongation (TE) of each specimen were evaluated according to tensile test results. Optical microscopy (OM), scanning electron microscopy (SEM) and transmission electron microscopy (TEM) techniques were applied in order to investigate the microstructural properties of selected specimens. Metallographic sample preparation procedure that covers grinding, polishing and etching steps were carried out for OM and SEM examinations. After grinding by using water-cooled silicon carbide papers with different grit-sizes, 9 µm and 1 µm diamond pastes were used for coarse and fine polishing. Then samples were etched with 4% Nital solution. For TEM examinations, continuously cooled samples were cut into small pieces, then grinding was performed until achieving a thickness about 100 µm. Then, jet polishing technique was applied by using a solution consists of 2% picric acid, 5% hydrochloric acid and ethanol. Additionally, extraction

replication, which is a commonly used sample preparation technique for TEM examinations that provides an opportunity to characterize nano-sized particles, was performed to analyze possible carbide precipitations in samples containing 1,4% silicon [26-28]. X-ray diffraction (XRD) technique was also applied to high silicon contented samples in order to verify the carbide-free structure. XRD samples were prepared as following the same metallographic sample preparation procedure applied to OM and SEM samples. XRD analyses were performed with Cu-Kα radiation at a scan rate of 1 °C/min.

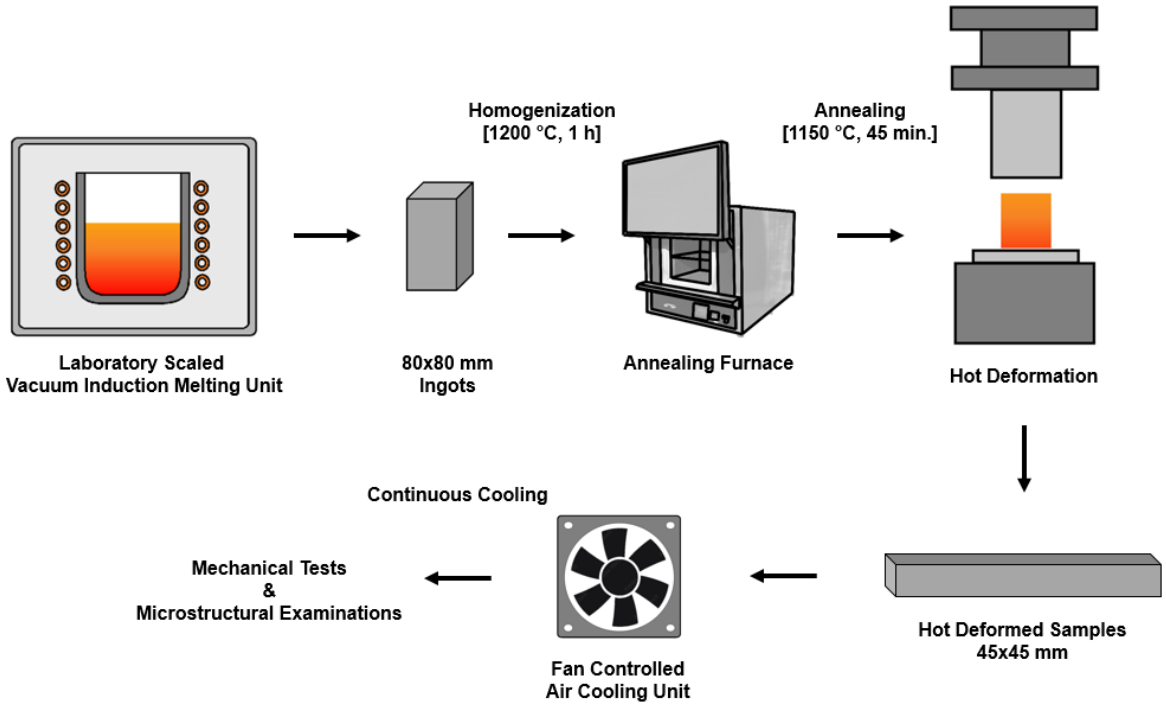

Figure 1. Production route of laboratory scaled experimental heats

2.2 Artificial Neural Network [ANN] Model

2.2.1. Network selection

MATLAB r2020b software was used for the construction and calculation of ANN model. The effectiveness of network-based prediction models relies on its network architecture and selected parameters. A Multi-Layer Perceptron (MLP) based feed forwarded ANN structure was proposed for the estimation of mechanical properties in this study. The MLP is one of the most common type of ANN and its topology consists of one or more hidden layer between input and output layers. The signals are received by input layer is transferred in forward direction to the nodes in hidden layers. Then each nodes performs a computation on received signal by using an activation function, and produces an output signal [29]. The purpose of using more than one hidden layer is generally related with decreasing the need of total number of nodes [30]. Depending on input parameters and complexity of the problem, it was decided that one hidden layer is a suitable selection for this study. The number of nodes in the hidden layer has a great influence on accuracy of training. It is known that, choosing too many nodes may cause an overfitting that means even a high performance acquired in training, insufficient response of network might be

observed in testing stage. On the contrary, if the hidden node number is selected fewer than the necessary, the training of network might be insufficient for learning. Although, there is no generalized approach or rule of thumb for selecting the number of hidden nodes, some suggestions were made in previous studies [31, 32]. These suggestions cover different calculation criteria such as "$(n+o)/2$", "$2n$" or "$2n+1$" where "n" and "o" are the size of input and output variables, respectively. In this study, optimum hidden node number was determined by comparing results of trials in the range of "1" to "$2n+1$".

Performance of each training, validation and test stages were calculated with Mean Squared Error (MSE) and Correlation Coefficient (R) according to Eq. 1 and Eq. 2, respectively;

$$MSE = \frac{1}{n}\sum_{i=1}^{n}(f(x_i) - y_i)^2 \tag{1}$$

$$R = \frac{\sum_{i=1}^{n}(f(x_i)-\overline{f(x)})(y_i-\bar{y})}{\sqrt{\sum_{i=1}^{n}(f(x_i)-\overline{f(x)})^2}\sqrt{\sum_{i=1}^{n}(y_i-\bar{y})^2}} \tag{2}$$

where n, y_i and $f(x_i)$ are the total number of data, corresponding output and predicted data, respectively. A total number of 10 tests were performed with each hidden neuron trials and average performance results were compared.

2.2.2. Data selection and pre-processing of data

The chemical compositions and cooling rates (CR) of each experimental conditions were served as input data while YS, UTS and TE were used as output data. A total of 174 sets of data were collected under varying conditions. The ranges of the data are given in Table 1.

Table 1. The variables in input and output data sets

Variable Description	Unit	Mean	Std. Dev.	Min.	Max.
Input					
Carbon (C)	w%	0,2150	0,0382	0,1300	0,3304
Silicon (Si)	w%	0,6320	0,4407	0,2223	1,5650
Manganese (Mn)	w%	1,6987	0,2612	0,5680	2,2552
Chromium (Cr)	w%	1,0640	0,2121	0,2603	1,8986
Molybdenum (Mo)	w%	0,1418	0,0745	0,0100	0,3094
Vanadium (V)	w%	0,0121	0,0098	0,0019	0,0960
Titanium (Ti)	w%	0,0158	0,0095	0,0002	0,0572
Niobium (Nb)	w%	0,0126	0,0148	0,0038	0,0510
Nitrogen (N)	w%	0,0083	0,0016	0,0038	0,0129
Boron (B)	w%	0,0018	0,0011	0,0001	0,0038
Cooling Rate (CR)	°C·s^{-1}	1,18	2,68	0,74	4,11
Output					
Yield Strength (YS)	MPa	678	79	344	959
Tensile Strength (UTS)	MPa	1080	124	611	1386
Elongation (TE)	%	13,9	1,9	10,1	25,5

Randomly selected 70% of input data set were used for training the network while other pair of 15% were used for validation and test stages. Generally, slower learning rate and weak convergence are observed when processing

data have more than one dimension and if the size ranges of variables are different. As shown in Table 1, the input and output data have variables with different size ranges. For example, the average content of Mn (1,6987%) is approximately one thousand times larger than the average content of B (0,0018%) in steel compositions. Likewise, there is a large numerical difference between strength and elongation values in the output variables. In order to reducing the impact of difference in magnitudes and improving the training stability, the used data were normalized within the range of 0 and 1 by using Eq. 3;

$$x_n = \frac{x - x_{min}}{x_{max} - x_{min}} \tag{3}$$

where x_n is the normalized value of the corresponding x; x_{max} and x_{min} are the maximum and minimum values of processing data, respectively.

2.2.3. Training and testing of network

The network was trained with Bayesian regularization backpropagation algorithm. The backpropagation performs an adjustment in model parameters after each forward pass by minimizing error of the network. Even though backpropagation is an effective method on minimizing of error, it may suffer from overfitting problem as explained before. In such a case, regularization can help to overcome this issue by decreasing or removing the requirement of extensive cross-validation [33]. As one of the most common regularization algorithm, Bayesian regularization enables to avoid overfitting and improves the generalization of back-propagated network structure [34]. A schematic view of network structure is given in Figure 2.

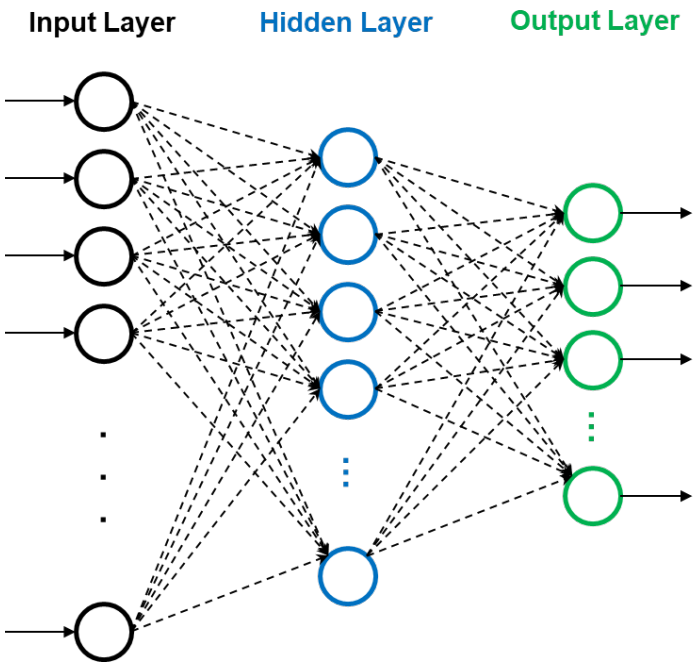

Figure 2. A schematic example of multi layered feed forwarded ANN

2.3 Multiple Linear Regression [MLR] Model

The input data used in training stage of ANN model was also selected for regression model calculations as the independent predictors for estimating mechanical test results. The predicted values of YS, UTS and TE were calculated separately for each dependent outcome and results were given in an equation format as shown Eq. 4;

$$Y = a_0 + a_1x_1 + a_2x_2 + a_3x_3 \ldots + a_nx_n \quad (4)$$

where Y is the predicted or expected value of the dependent variable, x_i is the independent variable or predictor and a_i is the calculated regression coefficient for each variable. Data normalization was also applied to MLR model to have comparable regression coefficients for each independent predictor.

2.4 Validating ANN and MLR Model with External Data Set

In order to verify the accuracy of the developed ANN and MLR model, a new data set consisting of chemical composition of low carbon steel and corresponding cooling rates extracted from experimental results of previous studies [35-37] and served to each model as input or independent predictor. The predicted results were compared with mechanical test results shared by authors in their research papers. Input and target variables of 27 new external data set are given in Table 2.

Table 2. The variables in input and target of external data sets

Variable Description	Unit	Mean	Std. Dev.	Min.	Max.
Input					
Carbon (C)	w%	0,2266	0,0254	0,1900	0,2800
Silicon (Si)	w%	1,3471	0,1941	1,1100	1,8310
Manganese (Mn)	w%	1,8331	0,3111	1,4800	2,4800
Chromium (Cr)	w%	0,6486	0,3791	0,0100	1,2000
Molybdenum (Mo)	w%	0,1096	0,0765	0,0060	0,2500
Vanadium (V)	w%	0,0084	0,0085	0,0030	0,0500
Titanium (Ti)	w%	0,0237	0,0095	0,0010	0,0330
Niobium (Nb)	w%	0,0250	0,0148	0,0021	0,0500
Nitrogen (N)	w%	0,0057	0,0020	0,0012	0,0080
Boron (B)	w%	0,0022	0,0011	0,0001	0,0033
Cooling Rate (CR)	$°C{\cdot}s^{-1}$	1,90	1,81	0,50	12,5
Output					
Yield Strength (YS)	MPa	906	129	662	1089
Tensile Strength (UTS)	MPa	1321	125	1054	1552
Elongation (TE)	%	10,9	3,3	5,0	16,2

III. RESULTS AND DISCUSSION

The ANN performances of various hidden neuron numbers are compared in Figure 3. It was seen that R results show a rising trend depending on the increment in the number of hidden nodes for the first eight trials, however all the correlation coefficients were resulted below 0,95 in this region. Even though relatively low significant differences were calculated, the overall performances became stable in trials with the number of hidden nodes nine and above. Based on the lowest MSE and the highest R results, eighteen hidden node was found as the best option

available as the overall performances compared. Therefore, a [11-1-3] network architecture with eighteen nodes in the hidden layer was purposed for the further study.

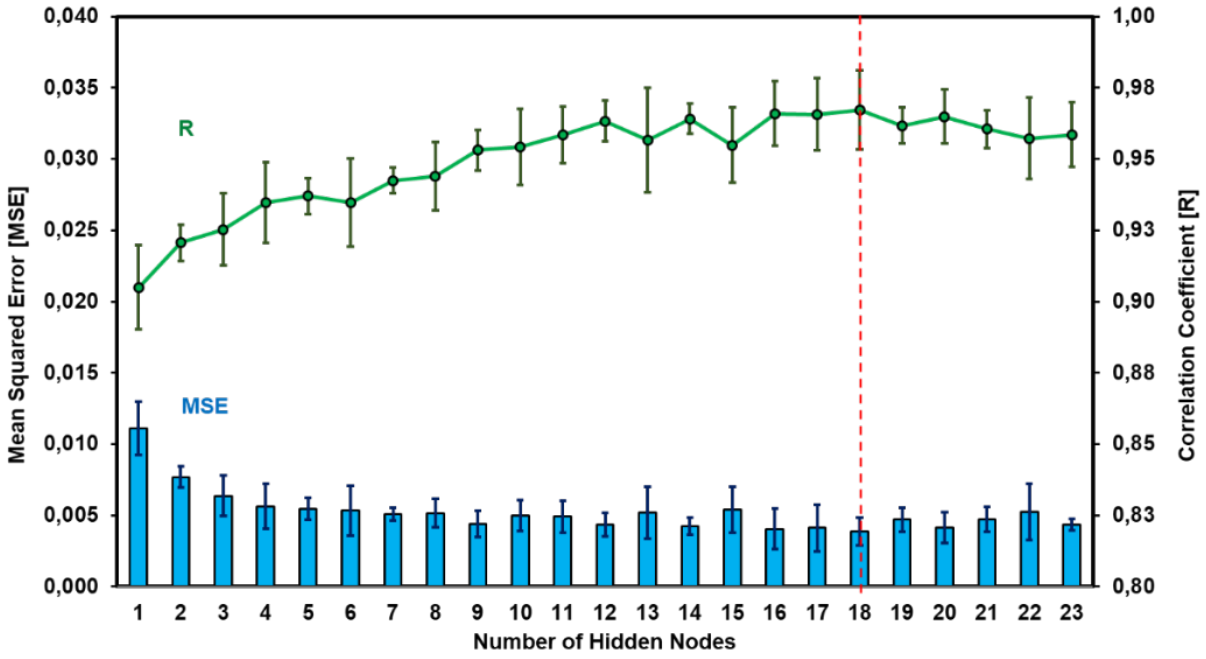

Figure 3. Performance results of ANN with various hidden nodes

The MLR analysis of the same selected variables used in the ANN model for YS, UTS and TE were resulted as follows;

$$\boldsymbol{YS} = -0{,}584 + 0{,}334[C] + 0{,}018[Si] + 0{,}640[Mn] + 0{,}748[Cr] + 0{,}061[Mo] + 0{,}131[V] + 0{,}215[Ti] - 0{,}107[N] + 0{,}064[Nb] - 0{,}012[B] + 0{,}321[CR] \quad (5)$$

$$\boldsymbol{UTS} = -0{,}644 + 0{,}376[C] + 0{,}011[Si] + 0{,}714[Mn] + 0{,}777[Cr] + 0{,}109[Mo] + 0{,}124[V] + 0{,}259[Ti] - 0{,}150[N] + 0{,}080[Nb] - 0{,}06[B] + 0{,}208[CR] \quad (6)$$

$$\boldsymbol{TE} = 1{,}11 - 0{,}215[C] + 0{,}003[Si] - 0{,}539[Mn] - 0{,}643[Cr] + 0{,}110[Mo] - 0{,}208[V] - 0{,}293[Ti] + 0{,}142[N] - 0{,}187[Nb] + 0{,}127[B] - 0{,}273[CR] \quad (7)$$

C is the main alloying element in steel and generally with the increasing C content; the hardness and the strength proportionally increase while the toughness decreases [38]. The correlation coefficient of C calculated positive for YS and UTS while negative for TE as its expected contribution explained above. Mn and Cr are commonly added to low carbon steel in order to retrieve the reduced strength due to lack of C content without compromising the

toughness. Additionally, the microstructural contribution of Mn and Cr in continuously cooled low carbon steels is to improve mechanical properties by promoting transformation of bainitic microstructure, which is relatively harder than ferrite and pearlite [39, 40]. The microstructural changes depending on the amount of Mn and Cr in the composition of laboratory scaled productions are shown in Figure 4. The increase of these elements provides a bainite dominant microstructure by suppressing ferrite and pearlite transformations as the steel cooled down from high temperature austenite region to room temperature, and helps to improve YS and UTS. This mechanism confirms the correlation coefficient calculation results of Mn and Cr for MLR model as the most effective input parameters enhancing YS and UTS.

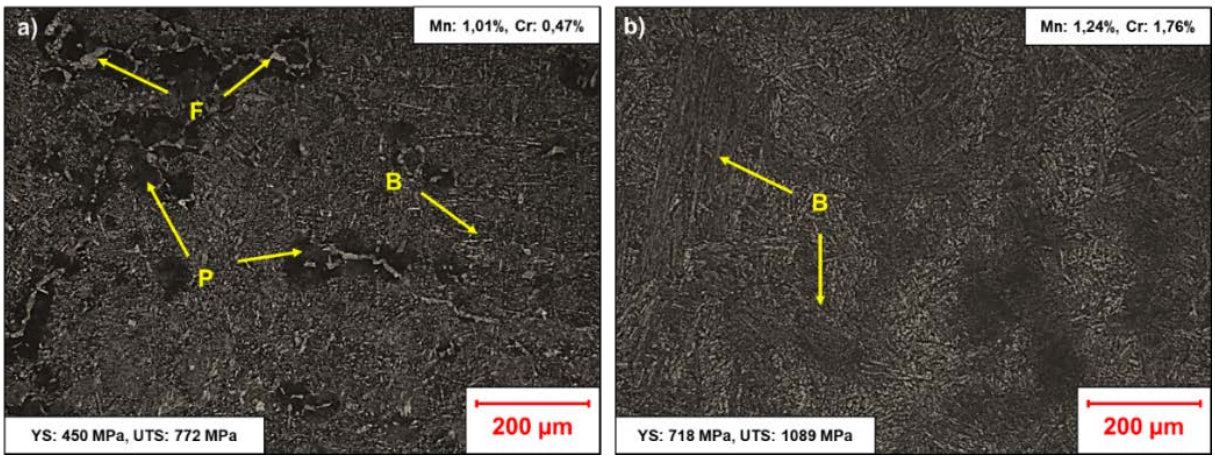

Figure 4. Optical microscope (OM) images of continuously cooled low carbon steel samples **(a)** lower Mn+Cr content **(b)** higher Mn+Cr content (F: ferrite, P: pearlite and B: bainite)

The major purpose of the addition of Si into continuously cooled steels is to retard the precipitation of carbides and provide a carbide-free microstructure, which is beneficial for mechanical properties of steel. The previous studies showed that carbide-free microstructure obtained with high Si addition helps to improve both strength and elongation properties of steel (41-43). TEM images of samples that have over 1,40% of Si confirm the absence of any carbide formations as shown in Figure 5. The dark field TEM image points out the presence of retained austenite on the edges of bainite plate while there is no sign of cementite or any other carbide formation around the bainitic microstructure. Additionally, X-ray diffraction (XRD) patterns shown in Figure 6 further confirm that only body-centered cubic (α) and face-centered cubic (γ) structured phases are present, without diffraction peaks of carbides detectable. According to MLR results, Si addition has a positive effect on both YS, UTS and TE, which supports the phenomena explained above. However, the magnitudes of the correlation coefficients of Si are calculated lower than its expected microstructural contribution. The bimodal shaped distribution of Si in data set is thought as to be the main reason for the lower correlation coefficients as shown in Figure 7.

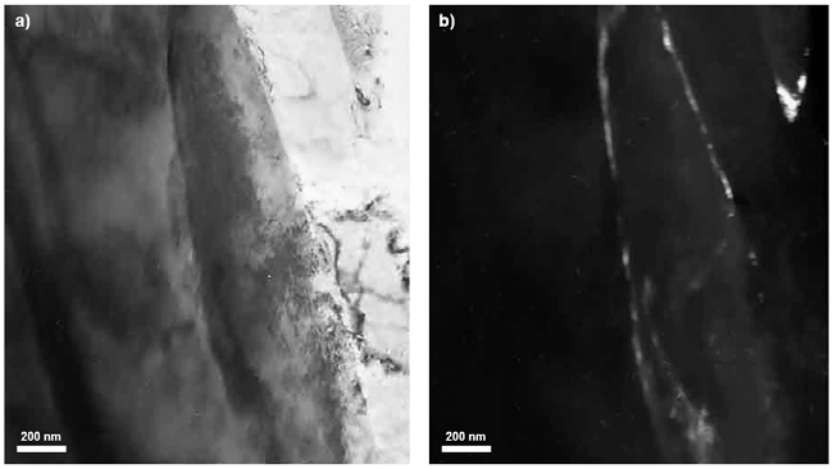

Figure 5. TEM images of sample with 1.44% silicon content **(a)** bright field image **(b)** dark field image

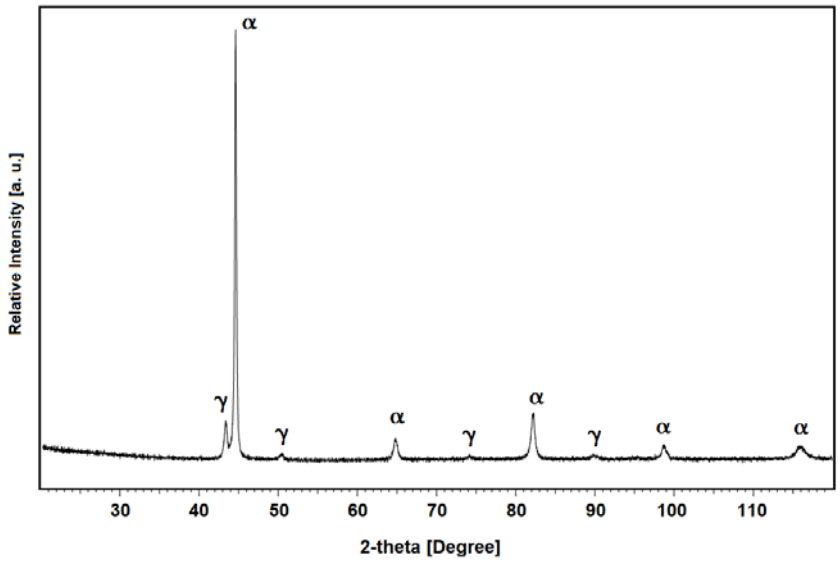

Figure 6. XRD patterns of sample with 1.44% silicon content

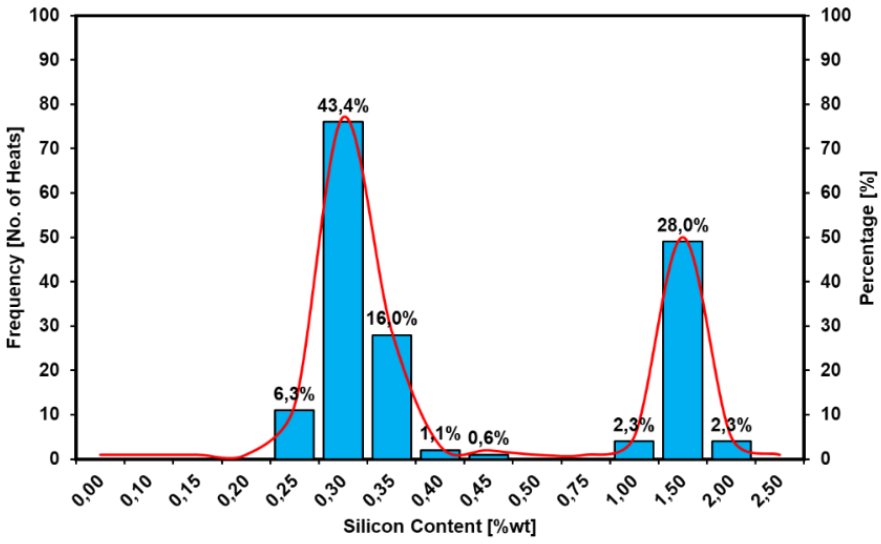

Figure 7. The bimodal distribution of Si contents of experimental heats

Similar to Si, MLR results showed that Mo addition also helps to improve both YS, UTS and TE. Previous studies indicated that a proper amount of Mo addition in continuously cooled low carbon steels provides an enhancement in strength by changing the microstructure from granular bainite to lath like upper bainite. Moreover, it was also reported that martensite/austenite (M/A) islands becomes finer with the addition of Mo which assists to improve elongation [44]. The effect of Mo to bainite morphology is confirmed with the SEM images as shown in Figure 8.

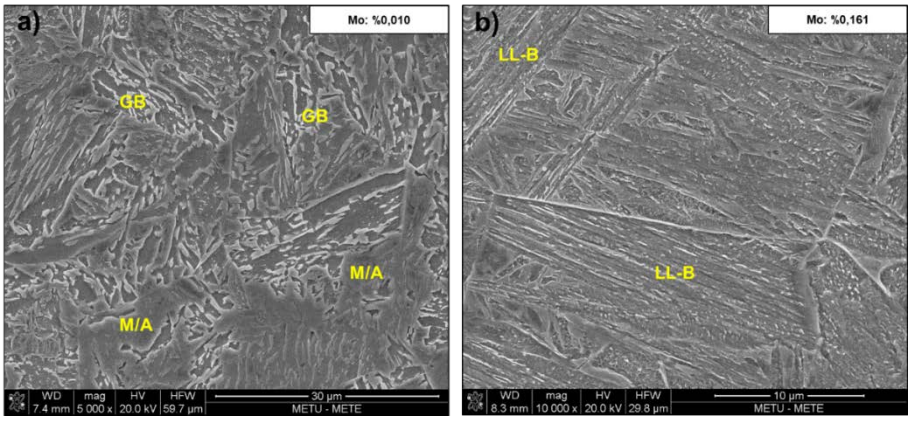

Figure 8. SEM images of continuously cooled low carbon steel **(a)** without Mo addition **(b)** with Mo addition (GB: granular bainite, LL-B: lath like bainite, M/A: martensite/austenite)

The significant positive contributions of micro-alloying elements such as Ti, Nb and V were also observed in MLR results. These elements are strong carbide, nitride and/or carbo-nitride formers and their influence on mechanical properties of continuously cooled low carbon steels by precipitation hardening and grain size refinement mechanism have been reported [45]. The prior austenite grain boundary (PAGB) sizes of trial heats with same cooling regime and chemical composition except Nb addition are compared in Figure 9. It is seen that the average grain size is decreased from 32,2 µm to 13,4 µm by adding 447 ppm Nb while YS and UTS increase 31,2% and 15,0%, respectively. As shown in Figure 10, Energy Dispersive Spectroscopy (EDX-SEM) results also confirmed the effective role of Nb precipitates in pinning mechanism of austenite grain boundaries and inhibiting the grain growth.

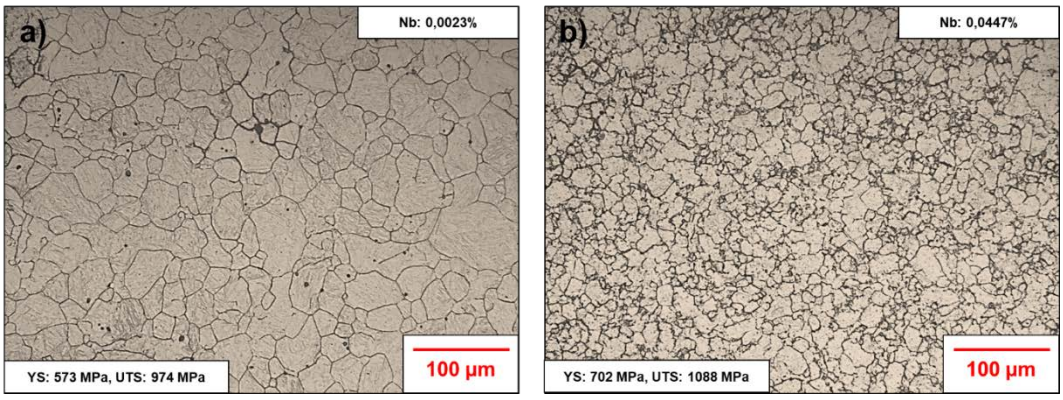

Figure 9. The comparison of PAGB sizes **(a)** without Nb addition **(b)** with Nb addition

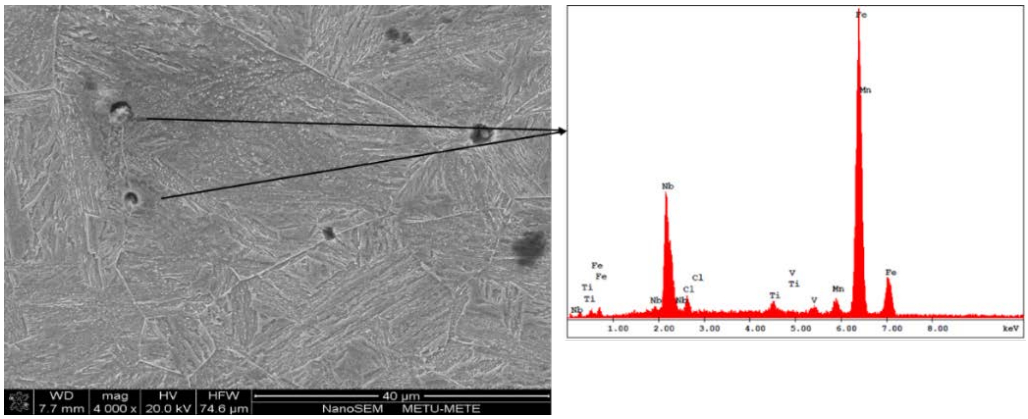

Figure 10. EDX-SEM results of Nb precipitates found in continuously cooled low carbon steel with 447 ppm Nb addition

The cooling rate (CR) has a strong effect on the transformation of austenite to different microstructural constituents resulting with the changes in mechanical properties [46]. It is possible to generate martensitic and/or bainitic microstructure instead of polygonal ferrite and pearlite by accelerating the CR which provides higher YS and UTS. Figure 11 shows the effect of CR on the microstructural changes for continuously cooled low carbon steel. It is seen that accelerating the CR from 0,74 °C/s to 2,40 °C/s enables bainite dominant microstructure by suppressing ferrite and pearlite for the same steel. The microstructural changes contribute an increment in both YS and UTS while TE decreases from 18,9% to 13,6%. The MLR result confirms the expected contribution of CR for both YS, UTS and TE.

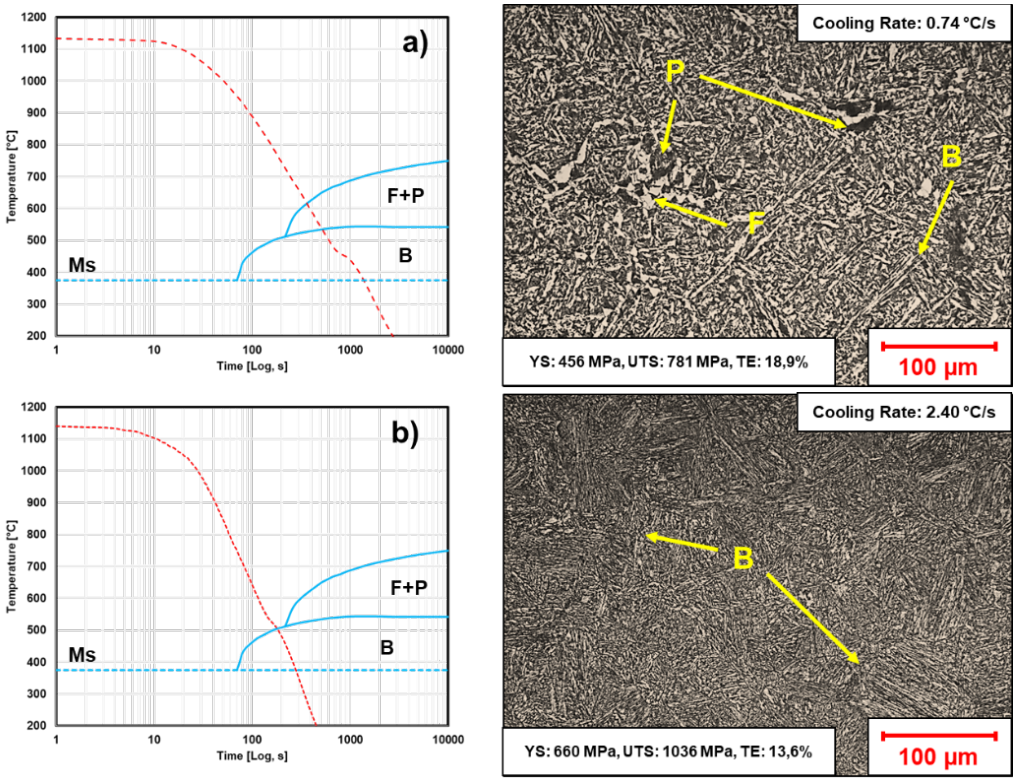

Figure 11. The microstructures of continuously cooled low carbon steel **(a)** lower cooling rate **(b)** higher cooling rate

In continuously cooled low carbon steels, the hardenability is increased by suppressing the nucleation of ferrite with even small amounts of B addition [47]. However, in order to benefit from its advantages on mechanical properties, B should be available as soluble atoms instead of precipitates at the grain boundaries [48]. For this purpose, a proper amount of Ti is generally added to molten steel in order to stabilize N and prevent B to precipitate as BN. Moreover, Mo and Nb additions are preferred to avoid grain boundary segregations of B element [49]. Nevertheless, in contrast to the explained phenomena, the correlation coefficient of B is calculated as negative for both YS and UTS while positive for TE in MLR model predictions.

In general, MLR performs a good correlation with expected microstructural effects on mechanical properties in case of significant differences for predominant predictors such as C, Mn, Cr and CR. However, when the phenomena is complex and needs to be evaluated by taking into consideration of all dependent parameters, as in the example of the effect of B addition in continuously cooled low carbon steels, MLR falls short of desired performance. Additionally, the individual indicators of each predictor strongly depends on the distribution of data, therefore any disordered shapes except uniform distribution as in the example of Si in this study might conduct to a misleading result.

Table 3. MSE and R performance results of ANN and MLR models

Performance Indicator	ANN Model [Overall]	ANN Model			MLR Model [Overall]	MLR Model		
		YS	UTS	TE		YS	UTS	TE
MSE	0,0030	0,0027	0,0027	0,0037	0,0090	0,0071	0,0062	0,0138
R	0,974	0,951	0,967	0,935	0,921	0,865	0,920	0,728

The overall MSE and R performance results of each output variable for the developed ANN and MLR models are given in Table 3. The ANN model shows a better prediction accuracy with lower MSE and higher R results compared to MLR model. The performance difference is more significant in TE prediction in which MLR model has the lowest R-value. Figure 11 also indicates a comparison of the data fitting both models to predict YS, UTS and TE. A better correlation was found between predicted and actual values for the ANN model compared to MLR model.

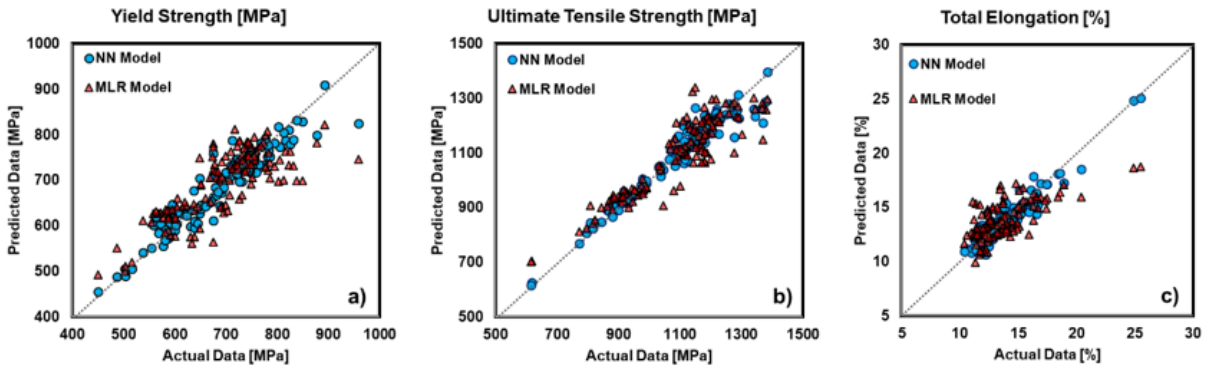

Figure 11. The prediction performance comparison of ANN and MLR models via data fitting **(a)** YS **(b)** UTS and **(c)** TE

The accuracy of the developed ANN and MLR models were also tested with 27 external data set extracted from previous studies. In order to compare the individual performance of each new data, Absolute Errors (AE) of each output and Mean Absolute Percentage Error (MAPE) of overall data were also calculated according to Eq. 8 and Eq. 9.

$$AE = \left|\frac{A_i - P_i}{A_i}\right| \tag{8}$$

$$MAPE = \frac{1}{n}\sum_{i=1}^{n}\left|\frac{A_i - P_i}{A_i}\right| \tag{9}$$

where n is the number of total data set, A and P values are the actual and predicted results, respectively. The predicted YS, UTS and TE values of ANN and MLR models with AE results for each new data set are given in Figure 12.

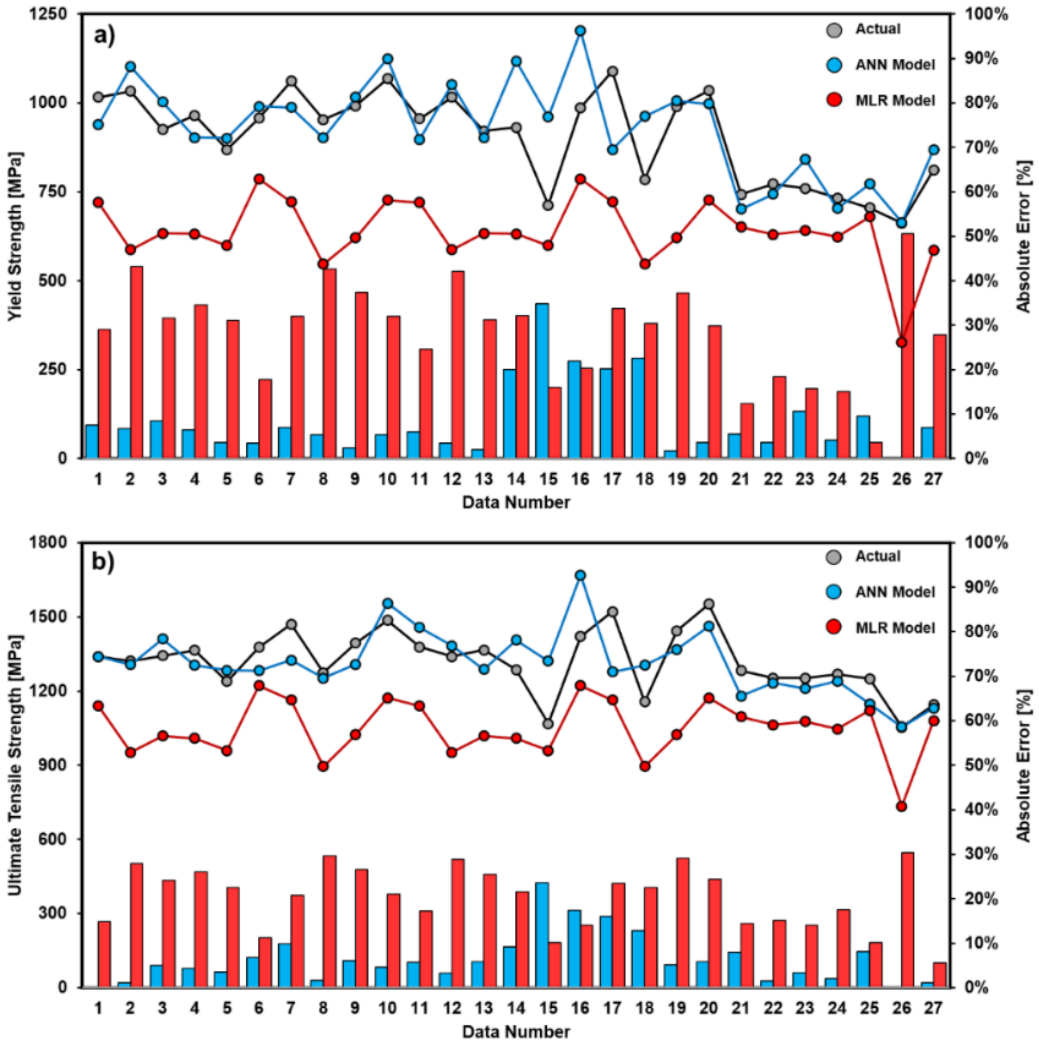

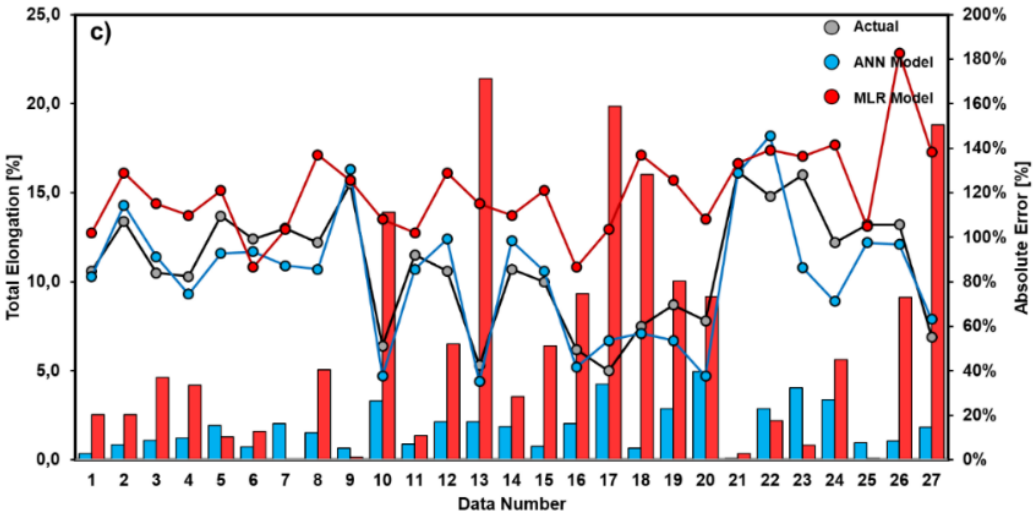

Figure 12. AE Performance results of ANN and MLR models with external data set **(a)** YS **(b)** UTS and **(c)** TE

The MAPE results of the models are given in Table 4. According to AE and MAPE results, better prediction accuracy with lower errors were calculated for YS and UTS compared to TE in both models. The possible reason behind of the poor prediction performance of TE for external new data is contributed with the limited distribution of values in a narrow range. Additionally, the chemical composition and cooling rates of new data set have some incompatible values with the input of experimental data set used in the developed ANN and MLR models. For example, Si and Mn contents of some new data are slightly higher than maximum value of experimental data while there are some other data that have lower Cr, Mo and CR than of those used for developing the models. Therefore, it is thought that the lower prediction capabilities might be arise from out-of-range data in the new data set. This assumption is also confirmed with the previous studies [50, 51] that report the outliers in test data may cause a significant decrease in prediction accuracy as the percentage and magnitude of the differences increase.

Table 4. MAPE results of ANN and MLR models with external data set

Performance Indicator	ANN Model			MLR Model		
	YS	UTS	TE	YS	UTS	TE
MAPE	8,6%	6,4%	14,9%	28,6%	20,3%	52,3%

In order to evaluate the prediction performance of models in detail, the external data was divided into two sub-groups. The first group was composed by selecting data that are completely included in experimental data set. The other group was consists of “unseen” data which have one or more out-of-range input value compared to data used for the training section. The newly categorized data sets are given in Table 5.

Table 5. The input and output variables of divided new data sets

Variable Description	Unit	Experimental Data		In-range Data		Out-of-range Data	
		Min.	Max.	Min.	Max.	Min.	Max.
Input							
Carbon	w%	0,1300	0,3300	0,2000	0,2600	0,1900	0,2800
Silicon	w%	0,2223	1,5650	1,1800	1,5400	1,1100	1,8310
Manganese	w%	0,5680	2,2552	1,4900	2,0200	1,4800	2,4800
Chromium	w%	0,2600	1,8986	0,3000	1,2000	0,0100	1,0020
Molybdenum	w%	0,0100	0,3094	0,0710	0,2500	0,0020	0,2290
Vanadium	w%	0,0019	0,0960	0,0048	0,0080	0,0010	0,0500
Titanium	w%	0,0002	0,0571	0,0100	0,0330	0,0010	0,0330
Niobium	w%	0,0038	0,0910	0,0150	0,0500	0,0010	0,0350
Nitrogen	w%	0,0037	0,0110	0,0059	0,0080	0,0012	0,0080
Boron	w%	0,0001	0,0038	0,0010	0,0033	0,0001	0,0033
Cooling Rate	$°C \cdot s^{-1}$	0,74	4,09	0,89	4,00	0,50	12,50

The MAPE results of new sub-divided data are shown in Table 6. Although a remarkably decrease especially in TE output was calculated, the MAPE results of MLR are still higher than of those error results of the developed ANN model. The MAPE results also indicate that the respond of the ANN model to new external test data remains stable even so the presented data includes one or more values that do not take part in the range of training data.

Table 6. MAPE results of ANN and MLR models with divided new data set

Model	All New Data Set [27 Data]			In-range Data Set [11 Data]			Out-of-range Data Set [16 Data]		
	YS	UTS	TE	YS	UTS	TE	YS	UTS	TE
ANN [MAPE]	8,6%	6,4%	14,9%	7,9%	7,2%	14,3%	9,2%	5,9%	15,3%
MLR [MAPE]	28,6%	20,3%	52,3%	22,0%	17,7%	32,9%	33,2%	22,2%	65,7%

IV. CONCLUSIONS

Based on the investigations of the present study, the following conclusions can be drawn;

- Depending on the magnitude and direction of the correlation coefficients, MLR model successfully predicted the effects of major predictor inputs such as C, Mn, Cr, Mo and CR on mechanical properties of steel in accordance with metallurgical aspects. However, the correlation coefficients of Si and B was calculated in conflict with their expected impacts by means of their microstructural contributions. This result indicates that the prediction capability of MLR model has a high dependency on uniform distribution of data. Furthermore, MLR model has a relatively low precision ratio when phenomena is complex and needs to be considered with more than one independent predictor.
- The MAPE results showed that the response of ANN model to new external data was found in better agreement with actual values compared to MLR model. In particular, the calculated errors in MLR model distinctively rises if the predicted data takes place in a narrow range.
- It was seen that even though the performance of MLR can be increased significantly by excluding out-of-range data from input predictors, the prediction accuracy remains lower than the developed ANN model results. However, the performance of ANN model resulted in a better accuracy with considerable stability even the newly tested input values are not included in training data set.
- In general, compared to MLR model, ANN model has not only better performance on predicting mechanical properties of continuously cooled low carbon steels but also its prediction accuracy can be enhanced by increasing the number of data with introducing external data set. It is thought that improved

prediction capabilities offers a good opportunity for reducing the production costs and the required time by minimizing the need of plant trials for new material development studies.

ACKNOWLEDGEMENTS

This research was supported by The Scientific and Technological Research Council of Turkey (TUBITAK) 1002-A Programme under the application number of 222M041.

REFERENCES

1. Schmitt JH, Iung T (2018) New developments of advanced high-strength steels for automotive applications. Comptes Rendus. Physique 19(8):641-56.
2. Lesch C, Kwiaton N, Klose FB (2017) Advanced high strength steels (AHSS) for automotive applications−tailored properties by smart microstructural adjustments. Steel Res. Int. 88(10):1700210.
3. Kwon O, Lee KY, Kim GS, Chin KG (2010) New trends in advanced high strength steel developments for automotive application. Mater. Sci. Forum 8(638):136-141).
4. Kučerová L, Jirková H, Mašek B (2016) Influence of Nb micro-alloying on TRIP steels treated by continuous cooling process. Manuf. Technol. 16(1):145-9.
5. Hasan SM, Ghosh M, Chakrabarti D, Singh SB (2020) Development of continuously cooled low-carbon, low-alloy, high strength carbide-free bainitic rail steels. Mater. Sci. Eng. A 771:138590.
6. Gomez G, Pérez T, Bhadeshia HK (2008) Strong bainitic steels by continuous cooling transformation. New Dev. Metall. Appl. High Strength Steels 1:571-82.
7. Gigović-Gekić A, Oruč M, Avdušinović H, Sunulahpašić R (2014) Regression analysis of the influence of a chemical composition on the mechanical properties of the steel nitronic 60. Mater Tehnol 48(3):433–437.
8. Chang J, Wang Z, Xiao T, Xin X (2018) Statistical Analysis of the Effects of Mn and Cr Contents on Mechanical Properties of Deformed Steel Bar. Proceedings of the 2018 International Conference on Mathematics, Modelling, Simulation and Algorithms (MMSA 2018), Chengdu, China, 25-26 March 2018. pp. 418-423.
9. Tumrate CS, Chowdhury SR, Mishra D (2021) Development of Regression Model to Predicting Yield Strength for Different Steel Grades. IOP Conf. Ser.: Earth Environ. Sci 796(1):012033.
10. Jones DM, Watton J, Brown KJ (2005) Comparison of hot rolled steel mechanical property prediction models using linear multiple regression, non-linear multiple regression and non-linear artificial neural networks. Ironmaking Steelmaking 32(5):435-42.
11. Sankar IB, Rao KM, Gopalakrishna A (2010) Optimization of steel bars subjected to Tempcore process using regression analysis and harmony search algorithm. Pak J Sci Ind Res 69:266-270.
12. Quiza R, Figueira L, Paulo Davim J (2008) Comparing statistical models and artificial neural networks on predicting the tool wear in hard machining D2 AISI steel. Int J Adv Manuf Technol 37:641.
13. Mukherjee I, Ray PK (2006) A review of optimization techniques in metal cutting processes. Comput Ind Eng 50(1-2):15-34.
14. Derin B, Alan E, Suzuki M, Tanaka T (2016) Phosphate, phosphide, nitride and carbide capacity predictions of Molten melts by using an artificial neural network approach. ISIJ Int 56(2):183.
15. He F, Zhang L (2018) Mold breakout prediction in slab continuous casting based on combined method of GA-BP neural network and logic rules. Int J Adv Manuf Technol 95:4081.
16. Jin X, Li C, Wang Y, Li X, Xiang Y, Gu T (2020) Investigation and optimization of load distribution for tandem cold steel strip rolling process. Metals 10(5):677.
17. Garcia-Mateo C, Capdevila C, Caballero FG, de Andrés CG (2007) Artificial neural network modeling for the prediction of critical transformation temperatures in steels. J Mater Sci 42:5391.
18. Nürnberger F, Schaper M, Bach FW, Mozgova I, Kuznetsov K, Halikova A, Perederieieva O (2009) Prediction of continuous cooling diagrams for the precision forged tempering steel 50CrMo4 by means of artificial neural networks. Adv Mater Sci Eng 10:2009.
19. Shah M, Das SK (2018) An artificial neural network model to predict the bainite plate thickness of nanostructured bainitic steels using an efficient network-learning algorithm. Adv Mater Sci Eng 27:5845.
20. Lee SI, Shin SH, Hwang B (2021) Application of artificial neural network to the prediction of tensile properties in high-strength low-carbon bainitic steels. Metals 11(8):1314.

21. Yemelyanov V, Yemelyanova N, Safonova M, Nedelkin A (2018) The neural network to determine the mechanical properties of the steels. In AIP Conf Proc 1952(1):020032.
22. Saravanakumar P, Jothimani V, Sureshbabu L, Ayyappan S, Noorullah D, Venkatakrishnan PG (2012) Prediction of mechanical properties of low carbon steel in hot rolling process using artificial neural network model. Procedia Eng 38:3418.
23. Somkuwar V (2013) Use of artificial neural network for predicting the mechanical property of low carbon steel. J Eng Comp App Sci 2(3):43.
24. Fujita T, Ochi T, Tarui T (2007) Prediction of hardness distribution in forged steel by neural network model. Nippon Steel Tech Rep 96:57-61.
25. Brownlee J (2020) Impact of dataset size on deep learning model skill and performance estimates. https://machinelearningmastery.com/impact-of-dataset-size-on-deep-learning-model-skill-and-performance-estimates/ Retrieved May 10, 2024.
26. Rolinska M, Gustavsson F, Hedström P (2022) Revisiting the applications of the extraction replica sample preparation technique for analysis of precipitates in engineering alloys. Mater Charact 189:111978.
27. Mukherjee T, Stumpf WE, Sellars CM (1968) Quantitative assessment of extraction replicas for particle analysis. J Mater Sci 3:127-135.
28. Kisakurek SE (1986) On application of the carbon extraction replica technique for the determination of second phase particles dispersed into metal matrix. Metall 19(1):19-25.
29. Jaiswal S (2024) Multilayer Perceptrons in Machine Learning: A Comprehensive Guide, https://www.datacamp.com/tutorial/multilayer-perceptrons-in-machine-learning. Retrieved May 10, 2024.
30. Stathakis D (2009) How many hidden layers and nodes?. Int J Remote Sens 30(8):2133.
31. Ding S, Li H, Su C, Yu J, Jin F (2013) Evolutionary artificial neural networks: a review. Artif Intell Rev 39(3):251.
32. Kaastra I, Boyd M (1996) Designing a neural network for forecasting financial and economic time series. Neurocomputing 10(3):215-236.
33. Hadzima-Nyarko M, Trinh SH (2022) Prediction of compressive strength of concrete at high heating conditions by using artificial neural network-based Bayesian regularization. J. Sci. Transp. Eng. 2(1):9-21.
34. Zhang X, Sun L (2021) Optimization of optical machine structure by backpropagation neural network based on particle swarm optimization and Bayesian regularization algorithms. Materials 14(11):2998.
35. Ackermann MA (2020) Bainitic TRIP Steels for Controlled Cooled Wire Rod, PhD Thesis. Universitätsbibliothek der RWTH, Aachen, Germany. 132 p.
36. Keskin B (2019) Bainitic transformation in low carbon micro-alloyed hot forged steels for diesel engine components, MSc Thesis, Middle East Technical University, Ankara, Türkiye. 87 p.
37. Zhou M, Xu G, Tian J, Hu H, Yuan Q (2017) Bainitic transformation and properties of low carbon carbide-free bainitic steels with Cr addition. Metals 7(7):263.
38. Hudok D (1990) Properties and selection: irons, steels, and high-performance alloys, Metals handbook, ISBN: 978-0-87170-377-4.
39. Ali M, Kaijalainen AJ, Hannula J, Porter DA, Kömi JI (2020) Influence of Chromium Content and Prior Deformation on the Continuous Cooling Transformation Diagram of Low-Carbon Bainitic Steels. Key Eng Mater 835:58-67.
40. Yao Z, Xu G, Hu H, Yuan Q, Tian J, Zhou M (2019) Effect of Ni and Cr addition on transformation and properties of low-carbon bainitic steels. Trans Indian Inst Met 72:1167.
41. Long X, Zhang F, Yang Z, Lv B. Study on microstructures and properties of carbide-free and carbide-bearing bainitic steels. Materials Science and Engineering: A. 2018 Feb 7;715:10-6.
42. Kumar R, Dwivedi RK, Arya RK, Sonia P, Yadav AS, Saxena KK, Khan MI, Moussa SB (2023) Current development of carbide free bainitic and retained austenite on wear resistance in high silicon steel. J Mater Res Technol 24:9171-9202.
43. Kaletin AY, Ryzhkov AG, Kaletina YV (2015) Enhancement of impact toughness of structural steels upon formation of carbide-free bainite. Phys Met Metallogr 116:109-114.
44. Hu H, Xu G, Zhou M, Yuan Q (2016) Effect of Mo content on microstructure and property of low-carbon bainitic steels. Metals 6(8):173.
45. Zhu M, Xu G, Zhou M, Hu H (2019) The Effects of Cooling Mode on the Properties of Ti–Nb Microalloyed High-strength Hot-rolled Steels. J Wuhan Univ Technol Mater Sci Ed 34(3):692.
46. Wang H, Cao L, Li Y, Schneider M, Detemple E, Eggeler G (2021) Effect of cooling rate on the microstructure and mechanical properties of a low-carbon low-alloyed steel. J Mater Sci 56:11098.
47. Altamirano G, Mejía I, Hernández-Expósito A, Cabrera JM (2012) Effect of boron on the continuous cooling transformation kinetics in a low carbon advanced ultra-high strength steel (A-UHSS). MRS Online Proc Lib 1485:83-88.

48. Ali M, Nyo T, Kaijalainen A, Javaheri V, Tervo H, Hannula J, Somani M, Kömi J (2021) Incompatible effects of B and B+ Nb additions and inclusions' characteristics on the microstructures and mechanical properties of low-carbon steels. Mater Sci Eng A 819:141453.
49. Da Rosa G, Maugis P, Portavoce A, Drillet J, Valle N, Lentzen E, Hoummada K (2020) Grain-boundary segregation of boron in high-strength steel studied by nano-SIMS and atom probe tomography. Acta Mater 182:226-234.
50. Klein BD, Rossin D (1999) Data quality in linear regression models: Effect of errors in test data and errors in training data on predictive accuracy. Info Sci 2:33.
51. Khamis A, Ismail Z, Haron K, Mohammed AT (2005) The effects of outliers data on neural network performance. J Appl Sci 5(8):1394.